

M.-D. Hua, P.C. De Vries, D.C. McDonald, C. Giroud, M.F. Johnson,
T. Tala, K.D. Zastrow and JET EFDA contributors

Scaling of Rotation and Momentum Confinement in JET Plasmas

"This document is intended for publication in the open literature. It is made available on the understanding that it may not be further circulated and extracts or references may not be published prior to publication of the original when applicable, or without the consent of the Publications Officer, EFDA, Culham Science Centre, Abingdon, Oxon, OX14 3DB, UK."

"Enquiries about Copyright and reproduction should be addressed to the Publications Officer, EFDA, Culham Science Centre, Abingdon, Oxon, OX14 3DB, UK."

Scaling of Rotation and Momentum Confinement in JET Plasmas

M.-D. Hua^{1,2}, P.C. De Vries³, D.C. McDonald³, C. Giroud³, M.F. Johnson³,
T. Tala⁴, K.D. Zastrow³ and JET EFDA contributors*

JET-EFDA, Culham Science Centre, OX14 3DB, Abingdon, UK

¹*Imperial College, SW7 2BY, London, UK.*

²*Ecole Polytechnique, Route de Saclay, 91128, Palaiseau, France.*

³*EURATOM/UKAEA Fusion Association, Culham Science Centre, Abingdon, OX14 3DB, UK.*

⁴*Association Euratom-Tekes, VTT P.O. Box 1000, 02044 VTT, Finland.*

** See annex of M.L. Watkins et al, "Overview of JET Results ",
(Proc. 21st IAEA Fusion Energy Conference, Chengdu, China (2006)).*

Preprint of Paper to be submitted for publication in Proceedings of the
35th EPS Conference on Plasma Physics, Hersonissos, Crete, Greece
(9th June 2008 - 13th July 2008)

1. INTRODUCTION

Rotation is believed to play a role in MHD stabilisation and turbulence suppression, thus affecting tokamak performance. This justifies studying momentum transport and its scaling with plasma parameters. A 600-entry database has been built at Joint European Torus (JET), aiming at identifying broad trends in rotation behaviour across plasma scenarios and revealing its possible influence on plasma confinement. Deviations from the trends may provide further insight in the physics that affect rotation. The toroidal plasma velocity is assumed to be that of the carbon ions measured by Charge Exchange spectroscopy. The torque delivered by Neutral Beam Injection (NBI) is the only rotation source considered in this paper.

2. ROTATION OF JET PLASMAS

Rotation is most conveniently described across plasma scenarios by the thermal and Alfvén Mach numbers as defined in [1]. Mach numbers are relevant to plasma turbulence and MHD stability, and they also ease cross-machine comparisons.

From the database, it was found that predominantly NBI heated plasmas in JET have a profile-averaged thermal Mach number, M_{th} , in the range $0.2 < M_{th} < 0.5$. Mean values in the database are $\langle M_{th} \rangle = 0.36$ for the Type I ELMy H-modes, $\langle M_{th} \rangle = 0.34$ for the Hybrid scenarios and $\langle M_{th} \rangle = 0.31$ for ITB shots. Type III ELMy H-modes exhibit a lower Mach number with $\langle M_{th} \rangle = 0.25$. Discharges with predominant Ion Cyclotron Resonant Heating (ICRH) rotate substantially slower: $0.03 < M_{th} < 0.14$. The dependence of the thermal Mach number on the ratio of torque to input power is shown in figure 1(a). The Alfvén Mach number, M_A , is one order of magnitude lower ($0.02 < M_A < 0.05$) and follows a similar trend. Despite a substantial torque input, M_A values in JET are comparable to the zero torque M_A values reported in [2].

Different Mach number profiles are observed: low density hot plasmas, such as ITB scenarios, exhibit peaked profiles, while profiles in high density, colder discharges such as ELMy H-modes are flatter. ICRH shots and counter NBI shots have flat or even hollow Mach number profiles. Figure 1(b) shows three characteristic JET M_{th} profiles. Differences in profile peakedness, p_{Mth} , could be explained by NBI torque deposition, which is located more off-axis for lower temperatures and higher densities. Indeed, p_{Mth} decreases with increasing n_e in figure 2(a). p_{Mth} is defined as the ratio of central to profile average Mach number. This effect is stronger for counter-NBI discharges, probably due to orbit effects in NBI deposition entailing a more off-axis torque profile. In figure 2(a), ICRH shots depart from the trend, possibly indicating that different torque or transport mechanisms prevail ([3]). The shape of the rotation profile plays an important role in plasma performance. For example, one of the damping models presented in [4] predicts that a flat rotation of $M_A = 0.02$ in ITER would stabilise the Resistive Wall Mode (RWM). While using the same model, however with a peaked profile, the mode can be unstable with a $M_A = 0.02$ rotation.

To further investigate rotation dependence on plasma parameters, regression analyses have been carried out on the Mach numbers. The best scalings were:

$$M_{th} \propto n_e^{-0.12 \pm 0.03} \cdot I_p^{+0.49 \pm 0.06} \cdot B_\phi^{-0.43 \pm 0.08} \cdot P_{in}^{-0.51 \pm 0.03} \cdot T_\phi^{+0.73 \pm 0.02} \quad \chi^2 = 1.11, \rho = 0.88 \quad (1)$$

$$M_A \propto n_e^{-0.08 \pm 0.04} \cdot I_p^{+0.80 \pm 0.08} \cdot B_\phi^{-1.12 \pm 0.12} \cdot P_{in}^{-0.36 \pm 0.04} \cdot T_\phi^{+0.95 \pm 0.04} \quad \chi^2 = 1.14, \rho = 0.84 \quad (2)$$

where n_e is the line-averaged density, I_p the plasma current, B_ϕ the central toroidal magnetic field, P_{in} the total heating power and T_ϕ the input torque from NBI. ρ is the Pearson correlation coefficient, which is unity for a perfect fit. χ^2 is the co-variance between the model and measured data, normalised to the measurement error. Provided the uncertainties are correctly estimated, this should be greater than unity, with best fit for $\chi^2 = 1$. As expected from its definition, the thermal Mach number scales positively with the rotation source, T_ϕ , and negatively with the heating source, P_{in} , consistent with the trend shown in figure 1(a). The Alfvén Mach number follows the same trend, although its definition does not involve the thermal energy. Both Mach numbers have a weak inverse dependence on density. They also strongly scale with the inverse safety factor, $q_{95}^{-1} \sim I_p/B_\phi$, especially M_A . The opposite dependence is reported in [2] for rotation with no external momentum source.

By definition, $(M_A/M_{th})^2 = \beta_\phi/3$, where β_ϕ is the ratio of kinetic to magnetic pressure. Since β_ϕ is also a measure of the stored energy, equations (1) and (2) suggest that there would be a positive scaling of stored energy with rotation

3. PLASMA CONFINEMENT

Besides the momentum sources, rotation is also determined by momentum confinement. It can be accounted for by means of the momentum confinement time, τ_ϕ , defined in [1]. Regression analyses on τ_ϕ and its counterpart for energy, τ_E , were carried out:

$$\tau_\phi \propto n_e^{+0.47 \pm 0.05} \cdot I_p^{+1.14 \pm 0.14} \cdot B_\phi^{+0.48 \pm 0.14} \cdot P_{in}^{-0.54 \pm 0.05} \quad \chi^2 = 8.54, \rho = 0.63 \quad (3)$$

$$\tau_E \propto n_e^{+0.41 \pm 0.02} \cdot I_p^{+0.76 \pm 0.08} \cdot B_\phi^{+0.26 \pm 0.07} \cdot P_{in}^{-0.40 \pm 0.02} \quad \chi^2 = 1.53, \rho = 0.78 \quad (4)$$

The parameter dependences in the τ_E scaling have the same directions as the ones in the IPB98(y,2) scaling, derived from the multi-machine International Confinement Database ([5]). They are however not identical. Both equations (3) and (4) show an inverse dependence on input power, which is consistent with turbulent transport theory. Although the τ_E fit quality is satisfactory, the τ_ϕ one is not, hinting that another parameter should be included. Given the possible role of rotation in confinement, torque was added to the scaling parameters:

$$\tau_\phi \propto n_e^{+0.48 \pm 0.04} \cdot I_p^{+1.03 \pm 0.10} \cdot B_\phi^{+0.15 \pm 0.11} \cdot P_{in}^{-0.33 \pm 0.06} \cdot T_\phi^{-0.10 \pm 0.03} \quad \chi^2 = 3.96, \rho = 0.74 \quad (5)$$

$$\tau_E \propto n_e^{+0.39 \pm 0.03} \cdot I_p^{+0.76 \pm 0.07} \cdot B_\phi^{+0.20 \pm 0.07} \cdot P_{in}^{-0.41 \pm 0.04} \cdot T_f^{+0.08 \pm 0.02} \quad \chi^2 = 1.48, \rho = 0.80 \quad (6)$$

In equation (6), t_E weakly scales with torque, consistent with an improvement of confinement by

rotation. Equation (5) however, shows a weakly decreasing momentum confinement with torque. The inclusion of torque improves the τ_ϕ fit quality substantially, while including other parameters did not, indicating that T_ϕ is relevant to confinement.

In equation (5) and (6), dependence of confinement on the rotation source is examined. The emphasis can be put on rotation itself, rather than on its source, by including the rotation in terms of M_A instead of T_ϕ . Such scalings benefit from the fact that, unlike T_ϕ and P_{in} , M_A and P_{in} are not correlated. This yields:

$$\tau_\phi \propto n_e^{+0.39\pm0.03} \cdot I_p^{+0.79\pm0.03} \cdot B_\phi^{+0.13\pm0.11} \cdot P_{in}^{-0.75\pm0.04} \cdot M_A^{+0.31\pm0.03} \quad \chi^2=3.70, \rho=0.78 \quad (7)$$

$$\tau_\phi \propto n_e^{+0.37\pm0.02} \cdot I_p^{+0.56\pm0.06} \cdot B_\phi^{+0.17\pm0.06} \cdot P_{in}^{-0.48\pm0.02} \cdot M_A^{+0.21\pm0.02} \quad \chi^2=0.99, \rho=0.86 \quad (8)$$

The fit quality for τ_E is much improved when including rotation in terms of M_A , possibly confirming the dependence of energy confinement on rotation. This was not observed in (6), maybe because of correlation between T_ϕ and P_{in} . Scaling (7) underestimates τ_ϕ in counter-NBI shots and overestimates it for the ICRH ones. In both these scenarios, either the transport itself differs, or the sources or their profile are not correctly accounted for.

In JET, the measured τ_E/τ_ϕ ratio is approximately unity, but varies from discharge to discharge, with $0.4 < \tau_E/\tau_\phi < 1.8$. Analysis of the core and edge confinement properties showed that this variation arises from core confinement differences ([1]). If transport is only diffusive, this is in disagreement with the turbulent transport prediction that core effective diffusivities are equal ([6]). The t_E/t_f spread does not seem to be a randomly distributed scatter, and in figure 2(b), τ_E/τ_ϕ decreases with M_A . This is consistent with the lower M_A coefficient in (8) than in (7). Again the ICRH scenario deviates from this trend. According to [7], the presence of a momentum pinch could explain the difference in core effective diffusivities, hence in confinement times. A higher pinch, resulting in a lower τ_E/τ_ϕ ratio, is predicted with a higher Mach number, which agrees with the trend observed here.

DISCUSSION

The rotation database enabled the identification of broad trends in different JET scenarios. The Mach numbers and their peakedness vary from one scenario to the other, the profile being usually flat with off-axis NBI. The energy and momentum confinement times seem to scale with torque or Mach numbers. Although close to unity, their ratio varies, showing a possible correlation with rotation ($0.4 < \tau_E/\tau_\phi < 1.8$). Deviations of ICRH and counter-NBI shots to these trends show the importance of profile effects which are not accounted for in the database.

The database enabled the derivation of scaling laws for the Mach numbers as well as for the momentum and energy confinement times, these must however be treated carefully. Operation of JET at similar safety factor values introduced a correlation between magnetic field and plasma

current. In addition, 60% of the entries, including almost all H-modes, have a fraction of NBI heating higher than 90%. NBI being the only torque source here, this means a coupling of input power and torque. These couplings are detrimental to the quality of the fits, and indeed, regressions carried out on the H-mode subset only proved unsatisfactory.

The inclusion of predominantly ICRH entries (NBI heating fraction lower than 70%) extended the P_{in}/T_ϕ range. Hybrid discharges and shots with Internal Transport Barriers (ITB) have a different heating scheme from baseline H-modes, hence further decorrelate P_{in} and T_ϕ . Nevertheless, even though including several plasma scenarios breaks the coupling between these parameters, it may well confuse the regression analyses by grouping very different confinement modes.

The presented database is restricted to JET operational range, meaning that the derived scaling laws are only valid in its vicinity. In particular, they do not enable any extrapolation to future devices like ITER. Furthermore, they do not contradict the IPB98(y,2) scaling: differences mostly arise from the lower quality of the JET database. This is due to higher parameter coupling, lower number of entries and smaller parameter space. The exclusive focus of the International Confinement Database on H-mode discharges is a source of further difference.

Further work at JET aims at improving the database quality by running experiments at higher ICRH fractions to reduce the coupling of torque and input power, and possibly identify rotation features characteristic to this heating scheme.

ACKNOWLEDGMENTS

This research was funded partly by the United Kingdom Engineering and Physical Sciences Research Council, the Ecole Polytechnique (Palaiseau, France), the British Council and by the European Communities under the contract of Association between EURATOM and UKAEA.. The views and opinions expressed herein do not necessarily reflect those of the European Commission. This work was carried out within the framework of the European Fusion Development Agreement.

REFERENCES

- [1]. de Vries P.C. *et al.* 2008 *Nucl. Fusion* **48** 065006
- [2]. Rice J.E. *et al.* 2007 *Nucl. Fusion* **47** 1618
- [3]. Eriksson L.G. *et al.* 2008 *this conference*
- [4]. Liu Y.Q. *et al.* 2004 *Nucl. Fusion* **44** 232
- [5]. McDonald D.C. *et al.* 2007 *Nucl. Fusion* **47** 147
- [6]. Mattor N. *et al.* 1988 *Phys. Fluids* **31** 1180
- [7]. Tala T. *et al.* 2007 *Plasma Phys. Control. Fusion* **49** B291

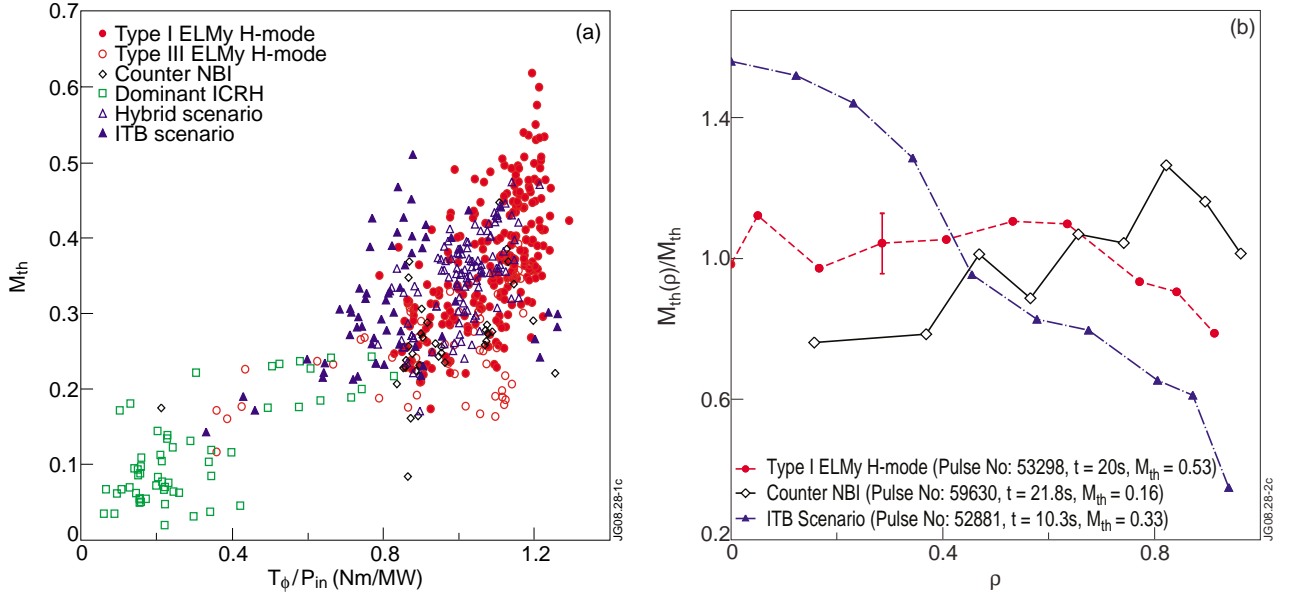


Figure 1: (a) The profile-averaged thermal Mach number, M_{th} , versus the ratio of the input torque, T_ϕ , to the heating power, P_{in} . (b) Local M_{th} value normalised to the profile averaged one, $M_{th}(r)/M_{th}$, as a function of square root of normalised poloidal flux, ρ , for three different scenarios. An errorbar typical of these profile is also shown.

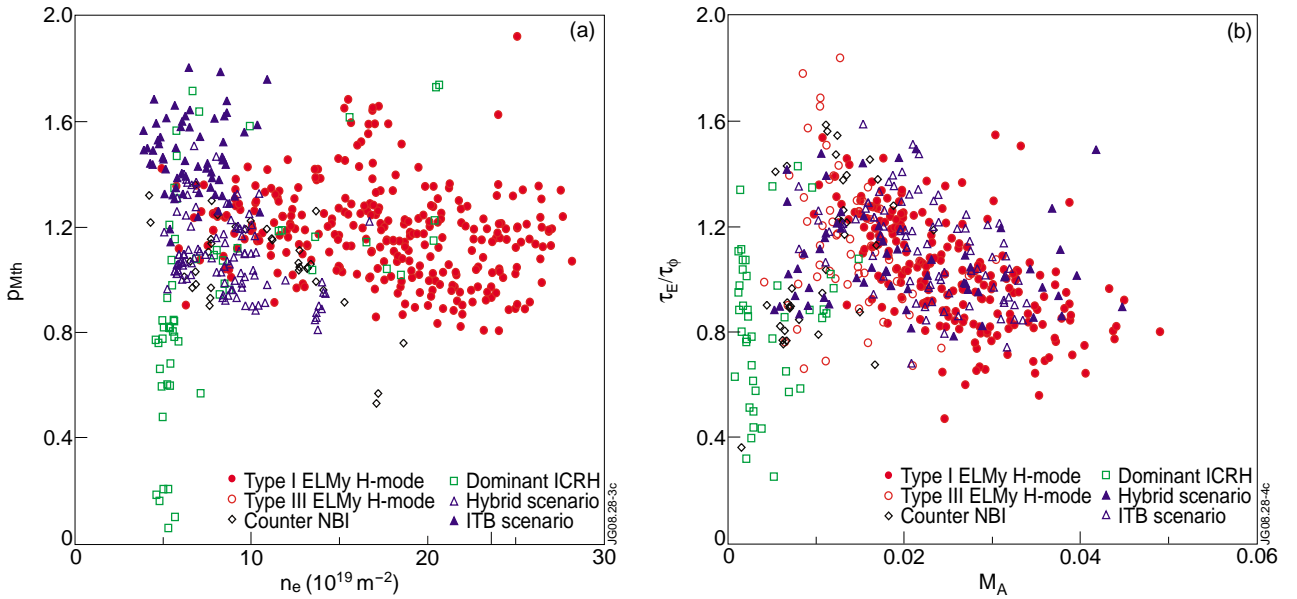


Figure 2: (a) The thermal Mach number peaking factor, p_{Mth} , ratio of the central and profile average values, against the line-integrated density, n_e . (b) The ratio of energy and momentum confinement time, τ_E/τ_ϕ , against the profile average Alfvén Mach number, M_A .